44P.

NASA CR-54047
EOS Report 4070-Final

SURFACE IONIZATION STUDIES

by

W. D. Dong, D. G. Worden, and D. Zuccaro

prepared for

NATIONAL AERONAUTICS AND SPACE ADMINISTRATION

CONTRACT NAS3-2592

EOS ELECTRO-OPTICAL SYSTEMS, INC., PASADENA, CALIFORNIA

Requests for copies of this report should be referred to

National Aeronautics and Space Administration
Office of Scientific and Technical Information
Attention: AFSS-A
Washington, D.C. 20546

NASA CR-54047
EOS Report 4070-Final

FINAL REPORT

SURFACE IONIZATION STUDIES

by

W. D. Dong, D. G. Worden, and D. Zuccaro

prepared for

NATIONAL AERONAUTICS AND SPACE ADMINISTRATION

11 June 1964

CONTRACT NAS3-2592

Technical Management
NASA Lewis Research Center
Cleveland, Ohio, 44135
Spacecraft Technology Division
Ross H. Hieber

ELECTRO-OPTICAL SYSTEMS, INC.
300 No. Halstead Street
Pasadena, California

193550

ABSTRACT

Tungsten, rhenium, and niobium were investigated to determine their surface ionization efficiencies for cesium, and to study the influence of adsorbed gases on the surface ionization of cesium. Cesium ion currents from wire samples of tungsten, rhenium, and niobium were measured as functions of wire temperatures and incident neutral cesium flux rates.

The experiments were performed with a cesium atomic beam apparatus designed by Electro-Optical Systems, Inc., under Contract NAS8-2546.

author

CONTENTS

ILLUSTRATIONS

TABLES

SUMMARY

An experimental research program in cesium surface ionization was conducted and the results are described. The program had two objectives: (1) to determine the surface ionization efficiencies of several refractory metals for cesium, and (2) to study the influence of adsorbed gases on the surface ionization of cesium.

Three refractory metals were investigated in the program: tungsten, rhenium, and niobium. Cesium ion currents from wire samples of these materials were measured as functions of wire temperatures and incident neutral cesium flux rates. Observed electron work functions and Richardson constants were determined for these three materials.

Cesium ionization efficiencies of tungsten and rhenium exceeded 99 percent. The ionization efficiency of cesium on niobium varied between 80 and 62 percent in the temperature range from $900^{\circ}K$ to $1,600^{\circ}K$.

Nitrogen adsorption results with the tungsten sample indicate that a coverage of about 25 percent of saturation will be present on a tungsten ionizer at $1,500^{\circ}K$ when the nitrogen pressure is $1 \cdot 10^{-6}$ torr. The rhenium data also agree qualitatively with other observations in the sense that the critical temperatures are lower on rhenium than on tungsten. However, the results imply a lower adsorption energy for cesium on rhenium than expected. Surface ionization experiments on niobium show that niobium has a relatively low surface ionization efficiency and hence should not be considered as a potential ionizer material.

1. INTRODUCTION

This is a summary report of an experimental research program in cesium surface ionization conducted by Electro-Optical Systems, Inc. for the National Aeronautics and Space Administration. The work was performed under Contract NAS3-2592 during the period 11 July 1963 to 11 January 1964.

The program had two objectives: (1) to determine the surface ionization efficiencies of several refractory metals for cesium, and (2) to study the influence of adsorbed gases on the surface ionization of cesium. Both objectives are related to the development of cesium ionizers for contact ion engines.

The significance of ionization efficiency to ion engine technology is its relation to engine lifetime. If an engine ionizer has an efficiency less than unity by only a fraction of a percent, the neutral cesium emitted by the ionizer can cause excessive electrode drain currents and sputtering, which, over a period of time, will severely impair engine operation. Since the projected uses of ion engines are mainly for extended space missions during which the engine must operate for thousands of hours, it is important to reduce neutral emission to an absolute minimum. The primary purpose of the ionization efficiency measurements of this program is to determine the ionization properties of new materials which are potentially capable of low neutral emission at high ion current emission.

The study of gas adsorption on ionizer materials is directed primarily to ionizer and ion engine testing. The vacuum environment in which engine tests are conducted is considerably different in gas composition and pressure than the environment of space. It is essential to know how the differences will affect ionizer performance. The

requirements for reliable testing can be determined only when the residual gases in test chambers are identified and their effects studied.

Three refractory materials were investigated in the program: tungsten, rhenium, and niobium. Cesium ion currents from wire samples of these materials were measured as functions of wire temperatures and incident neutral cesium flux rates. Tungsten was included as a reference material since its ionization properties have been studied extensively. Because of the importance of the electron work function of ionizers in ionization efficiency calculations, the work functions of the samples were determined also.

The experiments were performed with a cesium atomic beam apparatus designed by Electro-Optical Systems under Contract NAS8-2546. The apparatus was housed in a vacuum chamber operated at pressures in the 10^{-9} to 10^{-10} torr range. A mass spectrometer was used throughout the experiments to monitor the residual gases and to analyze the gases evolved from the metal samples.

Although atomic beam methods have been used in several prior investigations of ionization efficiencies, they have not been used for quantitative studies of cesium critical phenomena. Critical temperature determinations were attempted in this program and, where comparative data are available, the results agree very closely with measurements made by other methods.

2. GENERAL DESCRIPTION OF THE EXPERIMENTS

2.1 Surface Ionization Measurements

Measurements of the surface ionization efficiencies were made in a cesium atomic beam apparatus similar in its main features to the types used in several earlier experiments (Refs. 1, 2, 3, and 4).

A cesium atomic beam is produced by allowing cesium vapor in a small oven to effuse through a slit in the oven wall and pass through several cooled collimating slits located in line-of-sight positions. The vapor passing through the last cooled slit is a vapor stream with a cross section similar to the cross section of the slits. When the path of the vapor through the slits is long relative to the slit dimensions, the atoms in the vapor stream have velocities which are nearly unidirectional and thus form an atomic beam.

The collimating slits are arranged to direct the beam to a sample of the material under study. In the apparatus used in this program, the samples are wires mounted vertically with their axes perpendicular to the beam axis. The wires are surrounded by three colinear cylinders of equal radii, one which serves as an electron and ion collector from the central segment of the wire where the beam is directed, and the others serve as guard rings to maintain a uniform radial electric field at the wire surface. The central collector has an entrance slit for final collimation of the beam and an exit slit diametrically opposed to allow the portion of the beam not intercepted by the wire to pass through the collector.

When the cesium vapor flow through the source oven slit is effusive flow (that is, the cesium mean-free-path in its own vapor at the temperature and pressure in the oven is long relative to the oven slit dimensions), the beam intensity, q, in atoms cm^{-2} sec^{-1} at the

sample surface is

$$q = 9.66 \times 10^{20} \, pS_o/r^2T^{\frac{1}{2}}$$

where p is the saturated vapor pressure of cesium in the source oven (in torr), S_o is the source slit area (in cm^2), r is source slit-to-sample distance (in cm), and T is the oven temperature (in ^oK). Typical values of r in conventional beam systems designed for adsorption studies vary from 10 cm to 50 cm, the minimum distance being dictated by the space required for a good collimating slit system. In the system used in this program, r = 17.8 cm. At T = 380^oK, p = 1×10^{-3} torr (Ref. 5), so that q = 1.3×10^{13} atoms cm^{-2} sec^{-1} at r = 10 cm and q = 5.2×10^{11} atoms cm^{-2} sec^{-1} at r = 50 cm for a typical slit area of 2.5×10^{-2} cm^2. At higher source oven pressures, the intensity will be somewhat higher. However, at high source oven pressures, the cesium flow through the source slit is no longer effusive. Self-scattering of cesium in the source slit region diffuses the flow and the intensity becomes smaller than calculated with the equation above.

Ionization efficiency measurements are made in an atomic beam apparatus by comparing the cesium ion currents from the wire samples to the total incident flux of cesium to the wire. Let S be the area of the beam intercepted by the wire, and α, the sticking coefficient of cesium on the wire surface. Then αqS is the number of cesium atoms absorbed on wire surface per unit time. If I is the cesium ion current to the collector, I/e is the number of cesium ions desorbed from the wire per unit time. The ionization efficiency of the wire sample is then

$$\beta = I/e\alpha Sq$$

It is assumed that α is unity for cesium on the materials studied in this program. This has been shown to be true for tungsten (Ref. 6),

but there is very little information for other materials (Ref. 2). The determination of β thus involves three primary measurements: I, S, and q. The measurement of the collector current I is straightforward and S is calculated from the collector slit height and wire diameter. For the intensities calculated in the preceding paragraph, the current densities, I/S, are 2.2×10^{-6} and 8.3×10^{-8} amperes cm^{-2}, when α and β are unity. The corresponding currents for a 0.005-inch-diameter wire and a slit height of 1 cm are $2.8 \cdot 10^{-8}$ and $1.1 \cdot 10^{-9}$ amperes.

The determination of q is more difficult and is, in essence, an absolute beam intensity measurement. In several surface ionization experiments with atomic beams (Refs. 1 and 2) it has been common practice to rely on the high ionization efficiencies of surfaces with adsorbed oxygen to determine q. At some stage in the experiments, oxygen is introduced into the beam apparatus and permitted to adsorb on the sample surface. The ionization experiments are then performed with the oxygenated surfaces and it is presumed that, for these surfaces, $\beta = 1$. Under these conditions, the ion evaporation rate is equal to q and correlations of q with another experimental parameter, such as source oven temperature, is made for future or prior ion current measurements.

This procedure is often difficult to reproduce and is undesirable when oxygen is a specific surface contaminant to avoid. Moreover, there is no assurance that an oxygenated surface will provide an ionization efficiency of unity. It was for these reasons that the apparatus used in this program was designed to produce three simultaneous atomic beams. Two of the beams are directed to the wires of rhenium and niobium; the third beam is directed to a well-aged tungsten wire which serves as a standard reference surface for comparisons of ion currents.

This technique has merit for several reasons. Not only does it eliminate the need for introducing oxygen into the system, but, because ion currents can be measured simultaneously, differential measurements are possible. For low ionization efficiency materials, differential

methods are not required. However, when the ionization efficiency of a material approaches unity, it is simpler and more accurate to meter the difference between the specimen and standard ion currents than to meter each one separately. This procedure is possible, of course, only when the atomic beam geometries are equivalent and also when a common source oven is used for all beams; for it is obviously important that the beam intensities are identical and thermally coherent. Considerable care is necessary, therefore, in the design and assembly of the apparatus to provide equal atomic fluxes and equal beam interception areas for both wire samples and the tungsten standard.

2.2 Gas Adsorption Experiments

To determine the extent of contamination of the sample surfaces by the adsorption of residual gases from the vacuum system, several flash-filament experiments were performed with all samples.

The primary measurement of a flash-filament experiment is the pressure increase in the vacuum system when a sample surface is raised to a high temperature and the gases evolved from the surface contribute to the residual pressure of the system. At the beginning of run, a sample wire is heated to high temperature to clean the surface. After the initial cleaning, the wire is allowed to cool to some predetermined lower temperature where it is held for a time interval called the cold time. During the cold time, gases from the ambient are adsorbed. At the end of the cold time, the wire is flashed again to high temperature and the transient pressure increase in the systems noted. This procedure is repeated for several cold times (at the same lower temperature) which may vary from seconds to hours depending upon the types of gases being adsorbed and their partial pressures.

It is assumed that the maximum in the transient pressure increase observed during flashing is proportional to the amount of gas evolved from the sample surface and that the gas had accumulated on the surface during the preceding cold time. A plot of the maximum of

the pressure increase versus cold time for a series of flashes thus displays the rate at which the sample surface is becoming contaminated. Generally, during the early stages of adsorption on a clean surface, the amount of gas adsorbed increases linearly with time and consequently the pressure increases are linear with cold time. When the accumulation of the gas on the surface approaches an appreciable fraction of a monolayer, however, less gas is adsorbed per unit cold time. Subsequent adsorption then proceeds at a diminished rate and, finally, the pressure increases during flashing become constant and independent of cold time. When this is observed, the surface is said to be saturated.

Assuming the proportionality between the maximum of the pressure increase during flashing and the gas evolved remains constant, the ratio of the maximum, $\Delta p(t)$, to the final constant pressure increase, $\Delta p(\infty)$, is the fractional coverage of the surface, θ; that is,

$$\theta(t) = \Delta p(t)/\Delta p(\infty)$$

The function $\theta(t)$ is, of course, a function of the partial pressures of the contaminating gases and the temperature of the wire during the cold time. The partial pressures of the contaminating gases must be constant during the series of flashes and cold times required for a complete Δp versus t plot. It is possible in some instances to normalize readings taken at various pressures to a constant pressure, but this can be done only if the proper pressure dependence for the adsorption is known. For those diatomic gases which dissociate on the surface but desorb only in molecular form, the number adsorbed varies as $p^{\frac{1}{2}}$; for molecular or atomic adsorption with no dissociation, the number adsorbed varies linearly with p.

To use the preceding relation to determine $\theta(t)$, it is essential that the wire temperature during the cold time is sufficiently low for true saturation to occur. If the wire temperature is high, a

saturated layer of gas will not develop because desorption of the gas is occurring simultaneously with adsorption. Under these circumstances, when Δp becomes independent of cold time, it is an indication that a steady state coverage — a dynamic balance between adsorption and desorption — has been reached. This coverage is less than the saturated coverage.

The primary pressure indicator used in most flash-filament experiments is an ionization gage, suitably calibrated for the specific gas of interest. This is acceptable when the gas adsorbing is known and when contributions from other gases in the system are negligible. In this program, a mass spectrometer, capable of measuring partial pressures of 10^{-11} torr, was used during the flash-filament experiments to determine the specific gases adsorbed by the sample wires. The identity of the gases and their adsorption characteristics are discussed in the following subsections.

2.3 Electron Work Function

The electron work function of a material is an important parameter in surface ionization since it is the only surface parameter that appears in the Saha-Langmuir equation for ionization efficiency. It was measured for all three samples by the conventional method of determining the slope of the lines of log J/T^2 versus $1/T$ plots (Richardson plots), where J is the observed electron current density emitted at the temperature T. The work function obtained in this way is the observed work function, φ^{**}; the intercept of the Richardson line at $1/T = 0$ is the observed Richardson constant, A^{**}.

It is well known that calculations of ionization efficiencies with the Saha-Langmuir equation using φ^{**} will not predict results accurately for polycrystalline samples of materials (Ref. 7). Because of the variation in work function with crystal plane, a surface of a polycrystalline sample is composed of regions with different work functions. Observed ionization efficiencies are thus averages which

may differ from sample to sample of the same material depending upon the specific surface crystal orientations. The observed work function φ^{**} is itself an average, but it is weighted in favor of low work function planes whereas, for cesium ion emission, the high work function planes are equally important.

It has been shown (Ref. 8) that the effective work function of a surface, determined by electron emission measurements, is an appropriately weighted work function to use for ionization efficiency calculations for materials with high work functions on all planes. The effective work function, φe, is defined by

$$I = 120\, S_A T^2 \exp(-\varphi e / rT)$$

where I is the electron current (in amperes) emitted by the apparent surface area, S_A (in. cm^2). The effective work function is related to the observed work function and Richardson constant by

$$\varphi e = \varphi^{**} - 1.985 \cdot 10^{-4}\, T \log (A^{**}/120)$$

In Section 4, both φe and φ^{**} for the three materials are tabulated.

3. EXPERIMENTAL APPARATUS

A plan view of the beam apparatus is shown in Fig. 1. The cesium source oven, shown at the right in the drawing, is a tubular stainless steel enclosure with its axis along the beam axis. It is joined at a right angle to a similar tube to which the primary cesium supply line is coupled. Both tubes are heated by a tantalum sheath heater brazed to the tube walls. Cesium is introduced into the oven by crushing a glass ampule containing cesium and located in an oxygen-free, high-conductivity copper supply line. A fine stainless steel mesh in the line prevents glass from reaching the oven. Although separation has not been necessary, the copper line can be separated from the oven with a pinch-off tool which provides a cold-weld vacuum tight seal.

When the oven is heated, cesium effuses through the source slit located in a thin section of the oven wall facing the collimating slits. Three systems of collimating slits, accurately machined in copper plates and aligned with the source slit, collimate the vapor to form three cesium atomic beams with their axes separated by about 9 degrees. The copper plates are cooled by conduction through heavy copper mounting rods which are brazed to a liquid nitrogen cooled block. A shutter, actuated externally by a magnet, is located between the source slit and collimating slits to intercept the beam if desired. A vacuum line (not shown in the drawing), located directly below the shutter, is connected to the main vacuum manifold through a small reentrant liquid nitrogen trap.

The refractory materials under study are 0.005-inch-diameter wires mounted vertically (perpendicular to the plane of the drawing) in cylindrical diodes with their axes located on a 7-inch radius arc centered on the source slit. The wires are held in tension by leaf springs at their upper terminals (see elevation drawing of diode at

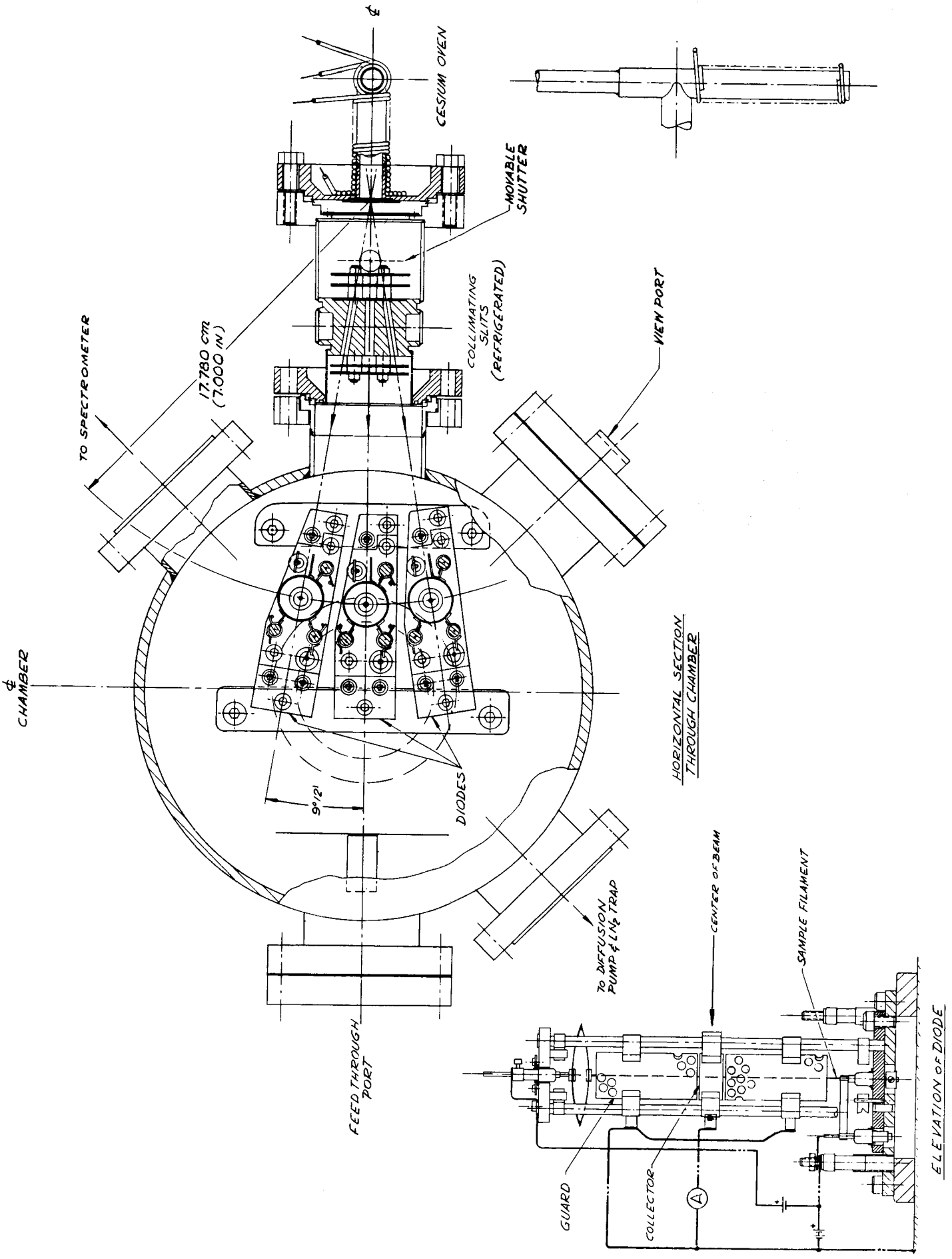

FIG. 1 CESIUM BEAM APPARATUS

lower left of drawing). Tension is adjusted during preliminary experiments. Typically, about 45 grams of tension are required initially to keep the wires aligned properly with the slit system when they are held at high temperatures. After aging, however, this tension is decreased somewhat.

The elevation drawing of the diode shows the location of the two guard cylinders and the collector cylinder surrounding a sample wire. The guard cylinders are perforated to allow extraneous cesium vapor to escape from the interior of the diode and reduce background ion currents.

The atomic beam enters the diode through an entrance slit in the collector cylinder. To prevent ions formed by the sample from leaving the collector through the entrance slit, a small plate (located to one side of the slit) is maintained at a positive potential with respect to the collector. The electric field deflects the ions to a projecting segment of the collector.

The three diodes are made as separate units and they can be removed from the chamber individually for reworking or examination. Each diode is located by locating pins which are rigidly fixed to the base of the chamber.

4. EXPERIMENTAL RESULTS

4.1 Work Function Measurements

Thermionic electron emission from the three wire samples to the central collectors of the diodes was measured as a function of wire temperatures for temperatures between 1,100°K and 2,500°K. The electron currents in this temperature range extended over nine decades.

The data are plotted in the Richardson plots shown in Figs. 2, 3, and 4. Different symbols for the data points indicate separate sets of measurements taken at various stages of the experiment. Current densities were computed from the measured currents and the apparent emitting area of the samples (product of wire circumference and length of central collector = $2.43 \cdot 10^{-2}$ cm^2). The wire temperatures were determined basically by optical pyrometry using emissivity and window absorption corrections. During the experiments, heating currents and voltages were metered. These data were converted to temperatures with temperature-resistance curves obtained in several preliminary pyrometric temperature determinations.

The observed work functions, φ^{**}, and Richardson constants, A**, obtained from the straight lines through the data points are given in the figures and in Table 1. The effective work functions for 1,000°K and 1,500°K, are shown also in the table.

TABLE 1

WORK FUNCTIONS AND RICHARDSON CONSTANTS FOR W, Re, AND Nb

	φ^{**} (ev)	A** ($amps/cm^2deg^2$)	φ_e(1,000°K) (ev)	φ_e(1,500°K) (ev)
Tungsten	4.72	66	4.77	4.80
Rhenium	5.15	760	4.99	4.91
Niobium	4.12	194	4.09	4.07

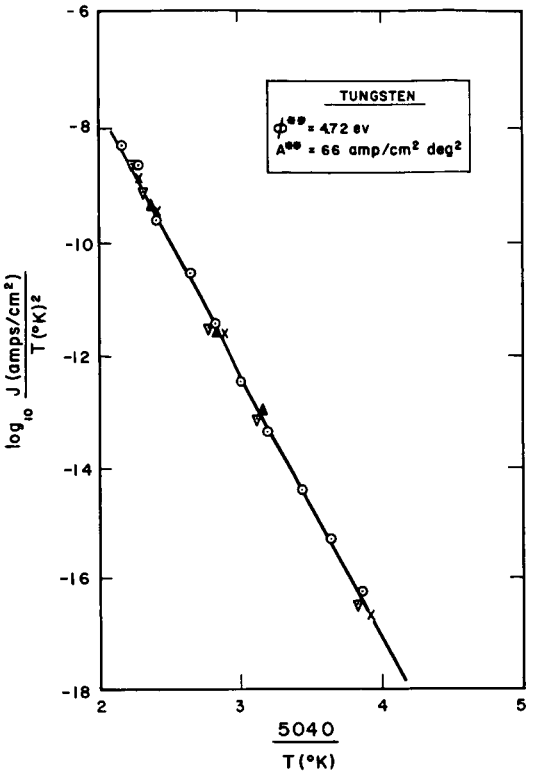

FIG. 2 ELECTRON EMISSION FROM TUNGSTEN

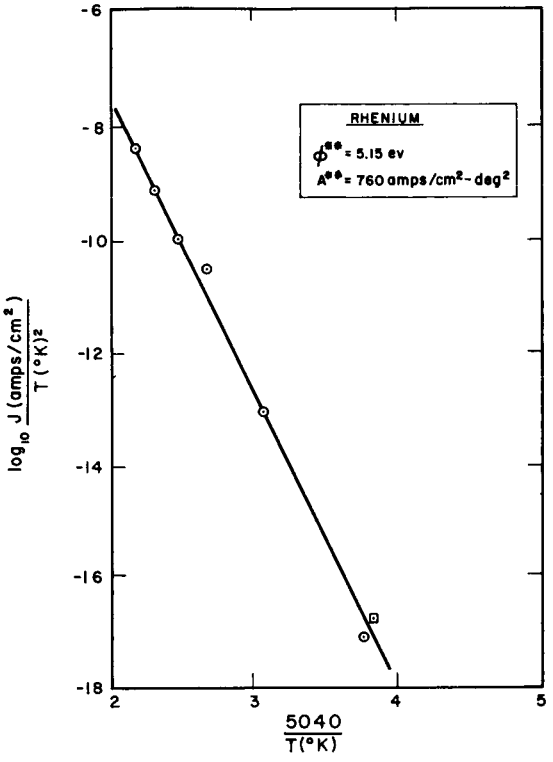

FIG. 3 ELECTRON EMISSION FROM RHENIUM

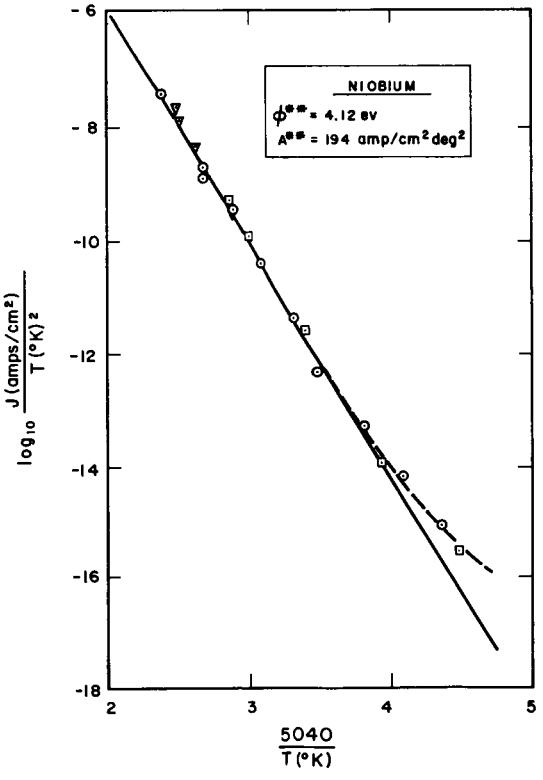

FIG. 4
ELECTRON EMISSION FROM NIOBIUM

Our observed work functions for all three materials agree with values given by other authors for wire samples. Taylor and Langmuir (Ref. 6)* quote 4.62 electron volts for tungsten compared to our 4.72 electron volts. Other published values for tungsten vary from 4.52 (Ref. 9) to 5.25 (Ref. 10). Rhenium is observed generally to have a higher work function than tungsten. Our value of 5.15 electron volts is in agreement with the 5.09 electron volts of Agte and his coworkers (Ref. 11) although our Richardson constant of 760 amps/cm^2deg^2 is greater than theirs by a factor of five. Levi and Espersen (Ref. 12) report an observed work function of 4.74 electron volts with a Richardson constant of 720 amp/cm^2deg^2.

Observed work functions for niobium are consistently between about 3.9 to 4.2 electron volts. Our observed work function is 4.12 electron volts with a Richardson constant of 194 amps/cm^2deg^2. Wahlin and Sordahl (Ref. 13) report 3.96 electron volts and 57 amps/cm^2deg^2; Riemann and Kerr-Grant (Ref. 14) quote 4.01 electron volts and 37 amps/cm^2deg^2. Because of these relatively low values, the ionization efficiency of cesium on niobium will be too low to be of interest for ion engines.

The electron emission from niobium at low temperatures was greater than the Richardson line drawn through the data points taken at higher temperatures. The reason for this difference is unresolved.

4.2 Gas Adsorption Experiments

The adsorption studies were conducted in two steps: (1) a mass analysis of the residual gases in the vacuum chamber, and (2) flash-filament experiments.

---

*Although not explicitly stated in this reference, the value quoted is an effective work function since the authors assume the Richardson constant of 120 amps/$cm^2{}^oK^2$.

4.2.1 Mass Analysis of Residual Gases

Early in the experiment, the total pressure in the vacuum chamber stabilized at $5 \cdot 10^{-9}$ torr with the apparatus running and the mass spectrum became nearly constant. Thereafter, only minor changes in the mass peaks were observed. A typical mass spectrum, taken at $5 \cdot 10^{-9}$ torr, is shown in Table 2. The major mass peaks were 14, 19, 28, and 40 amu; the minor peaks were smaller than the 28-peak by a factor of nearly 100 and therefore represent residual gas pressures in the 10^{-11} torr range. Since the spectrometer was uncalibrated, the partial pressure assignments shown in the third column of the table are approximate.

The 28 amu peak can be attributed to carbon monoxide (CO), molecular nitrogen (N_2), or ethene (C_2H_4). Since a typical hydrocarbon mass spectrum was absent, it is assumed that the ethene contribution to the 28 amu peak was negligibly small. The partial pressures of carbon monoxide and nitrogen are based on the height of the 12 amu (carbon) peak. It was assumed that the 12 amu peak originated entirely from an 8.5 percent dissociation of carbon monoxide by electron bombardment in the spectrometer ion source (Ref. 15). Thus, $P_{CO} = 35 \cdot 10^{-11}$ torr, and

$$P_{N_2} = P_{28} - (35 \cdot 10^{-11})$$

$$= 385 \cdot 10^{-11} \text{ torr}$$

If the 14 amu peak was due to a similar dissociation of molecular nitrogen, the dissociation fraction is 17/385 or 4.4 percent. This value is smaller than the expected fraction (Ref. 15) by a factor of three. Nevertheless, it is believed that the carbon monoxide and nitrogen partial pressure assignments are reasonable. Further evidence is presented in the discussion of the flash-filament experiments.

TABLE 2

MASS ANALYSIS OF RESIDUAL GASES

(Total pressure = $5 \cdot 10^{-9}$ torr)

Mass (amu)	Ion	Approximate Partial Pressure (torr x 10^{11})
12	C	3
14	N	17
15	CH_3	3
16	O	9
17	OH	2
18	H_2O	5
19	F	24
20	HF	2
28	N_2	385
	CO	35
29	$N^{14}N^{15}$, $C^{13}O$	3
40	Ar	11
44	CO_2	5

The 40 amu peak can be attributed unambiguously to argon which is not trapped effectively by liquid nitrogen. The 19 amu peak was found to be sensitive to the spectrometer operation and was due probably to residual contamination of spectrometer components by cleaning agents containing fluorine. The 19 amu peak height could be increased by a factor of 10 by operating a thoria-coated iridium filament in the spectrometer ion source. During normal spectrometer operation, a tungsten filament was used and the thoria-coated filament retained as an alternate.

4.2.2 Flash-Filament Experiments

The cold temperatures and flashing temperatures used in the flash-filament experiments are tabulated in Table 3. Other flash-filament experiments (not tabulated) with the tungsten sample were carried out at various stages of the experiment: the cold and flashing temperatures were usually 300°K and 2,000°K, respectively. Since the niobium wire was observed to bow severely at temperatures exceeding 1,660°K, the flashing temperature was kept below this value to avoid misalignment of the wire with the atomic beam slit system.

In all the tungsten and rhenium flash filament work, the only mass peaks observed to change during flashing were the 14 amu and 28 amu peaks which strongly implied nitrogen adsorption. There were no changes in the carbon, oxygen, water, fluorine, argon, and carbon dioxide. The apparent lack of desorption of oxygen, water, and carbon dioxide was not unexpected since these gases were minor constituents and the amounts that could adsorb during the cold times used in the experiments would be small compared to the amount of adsorbed nitrogen. Argon also would not be expected to adsorb in appreciable amounts because of its very low adsorption energy.

The absence of a change in the carbon peak is significant since it indicates that carbon monoxide was not adsorbed in significant amounts on the tungsten and rhenium samples. Judging from

TABLE 3

TEMPERATURES USED IN FLASH FILAMENT EXPERIMENTS

Sample	Cold Temperature (^{o}K)	Flash Temperature (^{o}K)
Tungsten	300	1,670
	300	2,000
	1,300	2,000
	1,480	2,000
	1,670	2,000
Rhenium	300	2,000
	1,135	2,000
	1,260	2,000
Niobium	300	1,660

the increases in the 28 amu peak during flashing of the tungsten sample, the carbon peak should have doubled during flashing if carbon monoxide were adsorbed in amounts corresponding to its assigned partial pressure contribution to the 28 amu peak (using the 8.5 percent dissociation fraction discussed above). Since this was not observed, the partial pressure for carbon monoxide shown in Table 2 must be too high or the simultaneous presence of both nitrogen and carbon monoxide changed the adsorption characteristics of these gases to favor nitrogen adsorption almost exclusively. In either case, it is reasonable to conclude that the predominant adsorbate was nitrogen.

4.2.2.1 Tungsten Flash-Filament Experiments

Two plots of the increase, $\Delta p(t)$, in the 28 amu peak during flashing of the tungsten sample versus cold time, t_c, are shown in Fig. 5. The peak increases are normalized to the constant peak increase, $\Delta p(\infty)$, observed when the surface became saturated after approximately a 15-minute cold time. The data taken during flashes from $300^{\circ}K$ to $1,670^{\circ}K$ are shown in the upper plot and those taken during flashes from $300^{\circ}K$ to $2,000^{\circ}K$ are shown in the lower plot. Although the maximum pressure increases during flashes to $2,000^{\circ}K$ were 40 times higher than the flashes to $1,670^{\circ}K$ (because of more rapid desorption) there is no evident difference in the Δp versus t_c characteristics. Both the initial slopes of the curves and the times required to reach saturated coverage are identical within experimental error.

Nitrogen adsorption on tungsten is atomic (Ref. 16); that is, the molecules dissociate on the surface and reside on the surface in atomic form. Desorption, however, occurs primarily in molecular form. Association of adsorbed atoms in two-dimensional binary collisions is thus an antecedent to desorption. As a result, nitrogen desorption occurs as a second order rate process. Despite this complexity, it can be shown that the number of atoms adsorbed varies linearly with time during the initial stages of adsorption (Ref. 17).

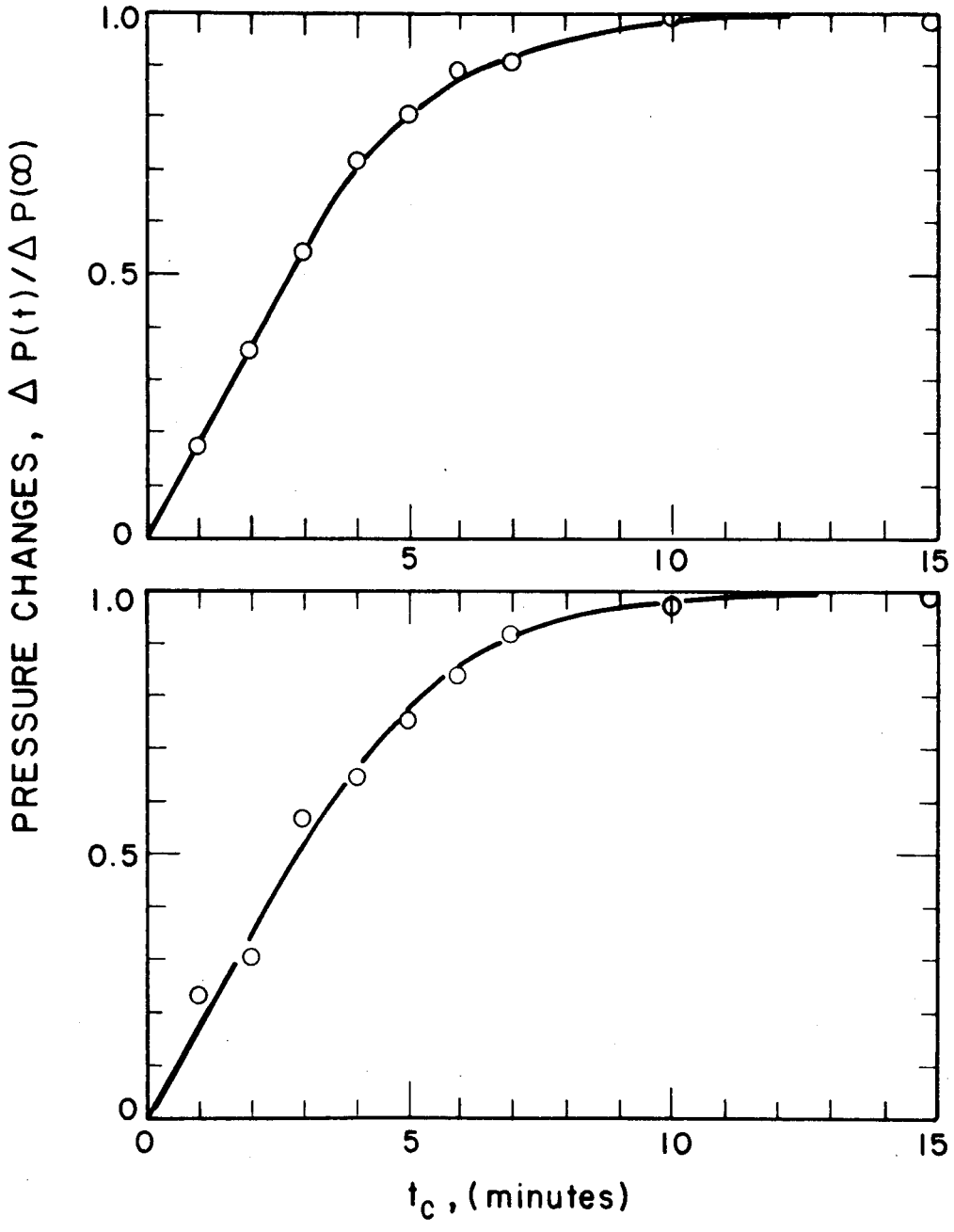

FIG. 5 NORMALIZED PRESSURE CHANGES, $\Delta P^{(t)}/\Delta P^{(\infty)}$ VS SAMPLE COLD TIME, t_c

The total number of molecules desorbed during flashing after a cold time, t_c, will be, therefore,

$$N_m = \alpha_m z_m S t_c$$

where α_m is the sticking coefficient for nitrogen molecules on tungsten, z_m is the number of nitrogen molecules incident on the surface per unit area and unit time, and S is the surface area. A fraction K of N_m will contribute to the pressure increase detected by the spectrometer during flashing. Thus,

$$\Delta p(t) = K \alpha_m z_m S t_c$$

When the surface is saturated with nitrogen,

$$N_m = N_{ms}$$

and since the fraction K will be detected by the spectrometer,

$$\Delta p(\infty) = K N_{ms}$$

or

$$\Delta p(\infty) = K n_{ms} S$$

where n_{ms} is the number of molecules adsorbed per unit area of the sample. The normalized pressure increases therefore are given by

$$\Delta p(t)/\Delta p(\infty) = \alpha_m z_m t_c/n_{ms}$$

It is assumed that the linear portion of the curves of Fig. 5 are represented by this equation.

The saturation time, t_s, is defined as the cold time required for $\Delta p(t)/\Delta p(\infty) = 1$ if the adsorption were linear. From the equation above

$$t_s = n_{ms}/\alpha_m z_m$$

z_m can be calculated with the kinetic theory expression

$$z_m = p / (2\pi mkT)^{1/2}$$

which, for nitrogen (Ref. 5), is

$$z_m = 4.02 \cdot 10^{20} \text{ p molecules/cm}^2 \text{ sec},$$

for p in torr. At the nitrogen partial pressure of $3.9 \cdot 10^{-9}$ torr shown in Table 2,

$$z_m = 1.6 \cdot 10^{12} \text{ molecules/cm}^2\text{sec}$$

The average t_s from the two curves of Fig. 5 is 338 seconds, therefore

$$n_{ms}/\alpha_m = z_m t_s$$

$$= 5.4 \cdot 10^{14} \text{ molecules/cm}^2.$$

Ehrlich (Ref. 18) and Eisenger (Ref. 17) report $\alpha_m = 0.3$ for low surface coverages although values as low as 0.1 (Ref. 19) and as high as 0.55 (Ref. 20) have been measured. Using $\alpha_m = 0.3$, we obtain

$$n_{ms} = 1.6 \cdot 10^{14} \text{ molecules/cm}^2$$

for the surface number density of nitrogen molecules in a saturated layer on the tungsten wire sample. Since nitrogen is adsorbed in atomic form, the significant number density is the atomic number density, n_{as};

$$n_{as} = 2n_{ms} = 3.2 \cdot 10^{14} \text{ atoms/cm}^2$$

The effective diameter of a nitrogen atom (1.42 angstroms, Ref. 21), is considerably smaller than the lattice constant of tungsten (3.16 angstroms, Ref. 21). If the adsorbed nitrogen atoms are located at those positions on the tungsten surface which are geometrically favored by "hard sphere" packing of nitrogen atoms on a crystallographic array of tungsten atoms, then the nitrogen surface atom density should equal the tungsten surface atom density for most of the low-index crystal planes expected to develop on a well-aged tungsten wire. It is noteworthy, therefore, that the nitrogen atom density, n_{as}, obtained in this experiment is smaller than the surface atom density of low-index tungsten planes. This result, observed also by others (Ref. 18), implies that nitrogen is preferentially adsorbed on special areas or sites on the tungsten surface. The nature of the favored adsorption sites is not known. Referring to Table 4, in which the tungsten surface atom densities are tabulated, the surface atom density of the 311 tungsten plane is very close to n_{as}. It is improbable, however, that the surface of the tungsten sample was composed solely of these planes. If a sticking coefficient of 0.55 were used in the calculation of n_{as} (instead of 0.3), n_{as} would be increased to $5.9 \cdot 10^{14}$ atoms/cm^2 and the 310 plane as well as those of lower surface atom density offer possible adsorption sites. However, the crystal planes in this group have work functions (see Table 4) which are too low to account for the measured work function of 4.72 electron volts.

TABLE 4

SURFACE DENSITIES OF TUNGSTEN ATOMS AND WORK FUNCTION FOR SEVERAL LOW-INDEX CRYSTAL PLANES

Miller Indices of Crystal Plane	Atom Density (atoms/cm^2)	φ (ev)
110	$14.1 \cdot 10^{14}$	> 4.70
100	10.0	4.56
211	8.2	4.69
310	6.3	4.35
111	5.8	4.39
411	4.8	-
210	4.5	-
221	4.0	-
311	3.7	4.55

TABLE 5

FRACTIONAL COVERAGE OF NITROGEN ON TUNGSTEN

Cold Temperature (^{o}K)	θ ($n_{as}=3.2 \cdot 10^{14}$ atoms/cm^2)	θ (Ref. 18) ($n_{as}=5.0 \cdot 10^{14}$ atoms/cm^2)
1,300	0.12	0.15
1,480	0.018	0.022
1,670	0.0046	0.0049

In addition to the flash filament experiments in which the cold temperature was 300°K, the tungsten sample was flashed to 2,000°K from 1,300°K, 1,480°K, and 1,670°K to determine the steady-state coverages at higher temperatures. The pressure increases during flashing were normalized to the pressure increase from a fully saturated surface to obtain the fractional coverage, θ, as discussed in Section 2. The results are shown in Table 5. Also shown in the table are calculated coverages using the results of Ehrlich. The agreement is excellent.

4.2.2.2 Rhenium Flash Filament Experiments

The rhenium flash filament data were qualitatively the same as the tungsten data except for the saturation time t_s. For rhenium, flashing from 300°K to 2,000°K, the saturation time was 1,160 seconds compared with the 338 seconds found for tungsten. This implies that either α_m is smaller or n_{ms} is larger on rhenium than the tungsten.

From the value of t_s obtained with rhenium

$$n_{ms}/\alpha_m = 18.6 \cdot 10^{14} \text{ molecules/cm}^2.$$

In Table 6, values of the nitrogen molecular surface density, n_{ms}, and atomic surface density, n_{as}, computed with this value of t_s, are shown for several values of α_m. There is no available information on either α_m or the degree of dissociation of nitrogen on rhenium. However, it is possible to place an upper limit on α_m from the data of Table 6 by comparing n_{ms} or n_{as} with the surface atom densities of various rhenium crystal planes. The surface densities for five low-index planes of rhenium are shown in Table 7. On the supposition that the nitrogen surface atom density cannot exceed the rhenium surface atom density and the planes tabulated will be the predominant planes exposed on the rhenium sample surface, it appears that the maximum α_m will be 0.8 if nitrogen adsorbs in molecular form and 0.4 if in atomic form.

TABLE 6

CALCULATED VALUES OF NITROGEN MOLECULAR AND ATOMIC SURFACE DENSITY

α_m	n_{ms} (molecules/cm^2)	n_{as} (atoms/cm^2)
0.2	$3.72 \cdot 10^{14}$	$7.44 \cdot 10^{14}$
0.4	7.44	14.9
0.6	11.2	22.4
0.8	14.9	29.8
1.0	18.6	37.2

TABLE 7

SURFACE DENSITIES OF RHENIUM ATOMS

Miller Indices of Crystal Plane	Atom Density (atoms/cm^2)
0001	$15.1 \cdot 10^{14}$
$10\bar{1}1$	14.3
$11\bar{2}0$	9.4
$10\bar{1}0$	8.1
$11\bar{2}2$	8.0

The rhenium sample was flashed from 1,135°K and 1,260°K to 2,000°K to determine the adsorption of nitrogen at high temperatures. Although there was appreciable scatter in the data, it is estimated that the coverage, θ, at 1,135°K was 0.066, and, at 1,260°K 0.0094. These coverages are considerably lower than those for tungsten at the same temperatures.

4.2.2.3 Niobium Flash Filament Experiments

The maximum temperature to which the niobium wire could be raised without endangering the sample alignment with the atomic beam slit system was 1,660°K. Despite a number of preliminary mounting attempts with various tensions, it was impossible to adjust the tension properly to preserve alignment at high temperature and, at the same time, avoid breaking the wire.

The sample was flashed to 1,660°K from room temperature for cold times varying from 1 to 30 minutes. In all instances, there were no increases in any mass peaks observed with the spectrometer. This result was unexpected, particularly in view of the departures noted in the electron emission data below 1,360°K.

Since nitrogen was the principal residual gas and would produce the largest changes in mass peak during flashing, the nitrogen peak was carefully scrutinized during several flashes. No evidence of adsorption could be detected. It is conceivable that nitrogen did not absorb on the niobium sample in detectable amounts if the sticking coefficient is very low. It is also possible that nitrogen was present on the surface either as an adsorbed species or as a nitride and was bound too tenaciously to the surface to evaporate at 1,660°K. If nitrogen evaporated as niobium nitride, it is improbable that it would have been detected with the spectrometer.

Adsorbed nitrogen has been observed to lower the work function of tungsten (Refs. 22 and 23). This suggests that it may have been adsorbed during the niobium electron emission measurements at low temperatures and caused a similar decrease in the niobium work function. Except for this evidence, however, the question of nitrogen adsorption on niobium remains unresolved.

4.3 Surface Ionization Experiments

The intensities of the three cesium atomic beams were markedly different notwithstanding their common source and the small angular separation of the beam axes. The differences could not be attributed to differences in ionization efficiencies of the three samples since the magnitudes of the ion currents were in the wrong order: the ion current from niobium was higher than the currents from tungsten and rhenium. Moreover, the differences were not constant but depended somewhat on oven temperature and also changed each time the source was heated. The differences have been ascribed to an incorrectly mounted slit plate which was located near the oven source. When it was coated with cesium, it effectively became a second source of cesium which contributed cesium to the beams.

All other features of the beam system were in proper order. Slit and sample alignment was checked before and after the experiment, there was no evidence of cesium clogging the source slit, and background currents in the system were sufficiently low to have no effect on measurements.

Because of the differences in beam intensities, it was not possible to measure ionization efficiencies on an absolute basis. Instead, the temperature dependences of the ion currents (for constant beam intensities) were used to define the limits of the efficiencies.

Within experimental uncertainty, when the beam intensities were constant, the ion currents from the tungsten and rhenium samples were constant for sample temperatures above the critical temperatures

to over 2,000°K. This result was expected on the basis of the work functions shown in Table 1. Using φ^{**} = 4.72 ev, the maximum calculated neutral fraction from tungsten at 2,000°K is 2 percent, or, an ionization efficiency of 98 percent. Since the minimum work function observed for the predominant low-index crystal planes of tungsten is 4.35 ev (see Table 4), the effective work function yields a better measure of the neutral fraction: for φ_e = 4.8 ev, the maximum neutral fraction from tungsten at 2,000°K is one percent. Using an effective work function of 4.90 ev, the cesium neutral fraction from rhenium is 0.6 percent at 2,000°K. There were no effects in the cesium ion currents from tungsten and rhenium that could be attributed to nitrogen adsorption although the lower temperatures of the tungsten measurements were well in the range in which nitrogen coverage was observed earlier to be high.

The cesium ion currents from niobium for a constant beam intensity (monitored by either the rhenium or tungsten samples) displayed a temperature dependence expected for a material with a low work function. To find the proper factor to convert cesium ion currents to ionization efficiencies, the ion currents were divided by several selected beam intensities and the resultant trial efficiencies compared with theoretical curves of efficiency versus temperature and work function. The best fit was obtained when the experiment of points were bounded by the 4.0 ev and 4.1 ev work function curves as shown in Fig. 6. It appears that the most suitable work function to use to characterize the ionization efficiency of the niobium sample is about 4.04 ev. This result agrees with the measured work function of 4.12 ev.

For comparison, the ionization efficiency of cesium on niobium was calculated using the effective work function (see Table 1) as a function of temperature. The resultant curve is labeled A in Fig. 6. The curve B was calculated using

$$\beta = 1 - 2 \exp (I - \varphi_e)/kT$$

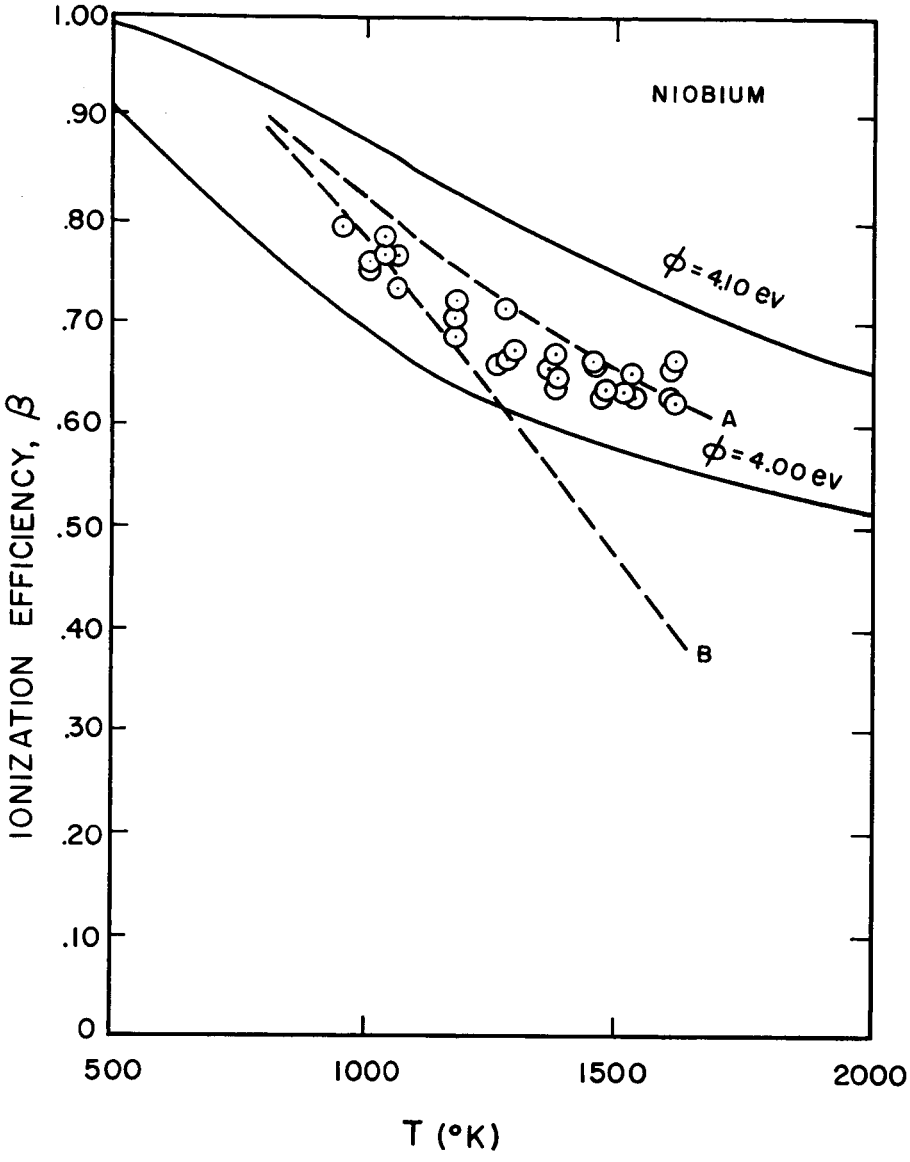

FIG. 6 CESIUM IONIZATION EFFICIENCY OF NIOBIUM

which is strictly applicable (Ref. 8) only for high work function materials. Neither curve displays the temperature dependence shown by the experimental points.

4.4 Critical Temperature Measurements

The critical temperature behavior of cesium ion currents from the three samples is shown in Figs. 7, 8, and 9. Both upper and lower critical temperature occurred with a perceptible burst of cesium ions and consequently was a more distinct transition than the lower critical temperature.

In Fig. 7, one lower and one upper critical temperature is shown for tungsten taken during runs at slightly different cesium beam intensities. The ion currents and ion current densities are in the same range as those measured by Taylor and Langmuir (Ref. 6) and our results agree closely. The upper critical temperatures observed in this experiment at two ion current densities are given in Table 8 with the corresponding critical temperatures of Taylor and Langmuir. The observations differ by only about $20^{\circ}K$ or 3 percent which is well within the variation expected in observations with different samples.

Two upper critical temperatures for rhenium and niobium are shown in Figs. 8 and 9. The rhenium critical temperatures were considerably lower than those for tungsten at comparable cesium ion current densities which is consistent with the results of others (Ref. 8). The niobium critical temperatures appear to be approximately the same as those for tungsten.

TABLE 8

OBSERVED AND CALCULATED (REF. 6)
UPPER CRITICAL TEMPERATURES

J $(amps/cm^2)$	$T_{observed}$ $(^{\circ}K)$	$T_{calculated}$ $(^{\circ}K)$
$2.9 \cdot 10^{-9}$	840	818
$2.4 \cdot 10^{-8}$	887	864

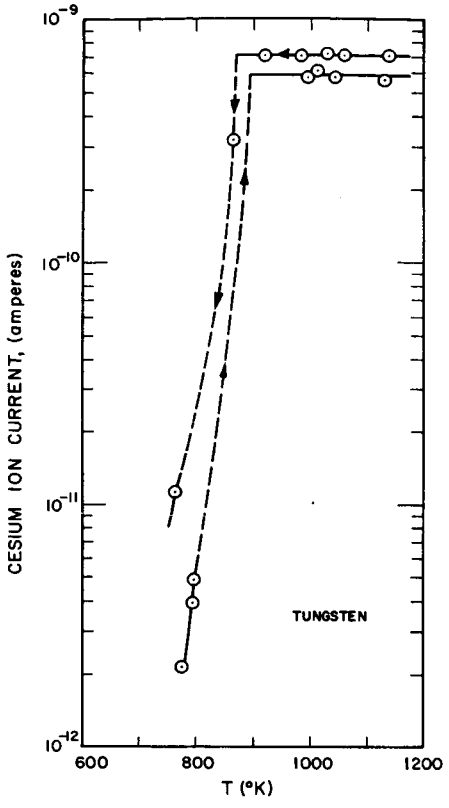

FIG. 7 CRITICAL TEMPERATURE CHARACTERISTICS OF CESIUM ON TUNGSTEN

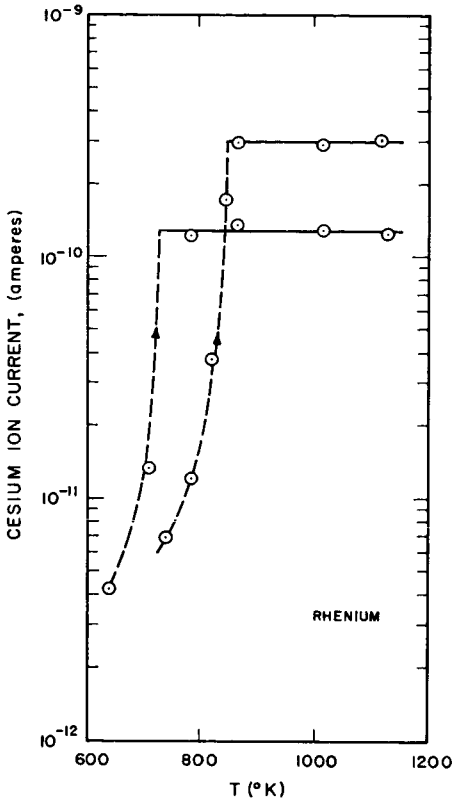

FIG. 8 CRITICAL TEMPERATURE CHARACTERISTICS OF CESIUM ON RHENIUM

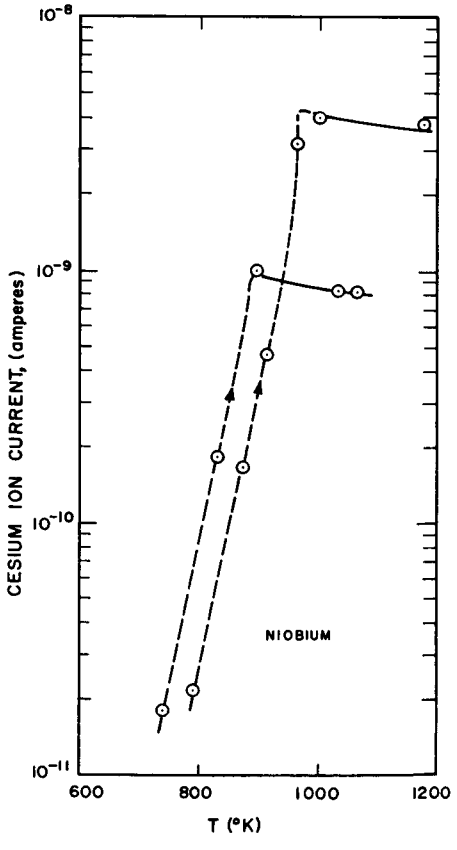

FIG. 9

CRITICAL TEMPERATURE CHARACTERISTICS OF CESIUM ON NIOBIUM

5. CONCLUSIONS

The main results of the experiment can be summarized as follows:

1. The observed electron work functions and Richardson constants for the three refractory wire samples are:

Tungsten: $\varphi^{**} = 4.72$ ev , $A^{**} = 66$ amps/cm^{2}deg^2

Rhenium: $\varphi^{**} = 5.15$ ev , $A^{**} = 760$ amps/cm^{2}deg^2

Niobium: $\varphi^{**} = 4.12$ ev , $A^{**} = 194$ amps/cm^{2}deg^2

These results agree well with those of other investigators.

2. Nitrogen was the major residual gas in the vacuum system. The total pressure in the system during the experiments was $5 \cdot 10^{-9}$ torr; the nitrogen partial pressure was $3.9 \cdot 10^{-9}$ torr. At this partial pressure, the nitrogen coverage on tungsten was 12 percent at a tungsten temperature of 1300°K and less than 1 percent on rhenium at 1260°K. Our results on nitrogen adsorption on niobium were inconclusive; either nitrogen did not adsorb on the niobium sample or the flash temperature of 1660°K was too low to effectively evolve nitrogen and provide a detectable signal in the mass spectrometer.

3. Judging from the temperature dependences of the cesium ion currents from tungsten and rhenium, the cesium ionization efficiencies of these materials exceeded 99 percent. This is consistent with the work function data. The ionization efficiency of cesium on niobium varied between 80 percent and 62 percent in the temperature range from 900°K to 1600°K.

4. Critical temperature behavior was observed at ion current densities of the same magnitude as those measured by Taylor and Langmuir. The upper critical temperatures for cesium on tungsten were in good agreement with the results of Taylor and Langmuir. Critical temperatures were considerably lower for cesium on rhenium than for cesium on tungsten

at comparable ion current densities. Niobium critical temperatures were in the same range as the tungsten critical temperatures.

The nitrogen adsorption results with the tungsten sample agree very closely with the results of Ehrlich, both in the temperature dependence of surface coverage and in the observation that nitrogen saturation at room temperature occurs with relatively few atoms per unit area compared with the surface atom density of tungsten. If it is assumed that nitrogen saturation of a sintered tungsten ionizer occurs with the same nitrogen atom density, then the data from this experiment, as well as from Ehrlich's work, indicates that a coverage of about 25 percent of saturation will be present on a tungsten ionizer at 1500°K when the nitrogen pressure is $1 \cdot 10^{-6}$ torr. This high value may be misleading, however, in relation to ionizer performance, for the simultaneous presence of cesium and nitrogen will affect the adsorption of both species on the ionizer surface and coverages may be lower. Moreover, on the basis of the total number of adsorption sites available (on a hard-sphere model, as discussed in Section 4), 25 percent of saturation may represent only about a 5 percent coverage of the total surface. It is significant that our ion current measurements at low temperatures revealed no effects attributable to nitrogen adsorption.

Quantitative measurements of critical temperatures by atomic beam methods have not been attempted before and the excellent agreement between the results on tungsten obtained in this experiment and the results of Taylor and Langmuir are encouraging.

The rhenium data also agree qualitatively with other observations in the sense that the critical temperatures are lower on rhenium than on tungsten. However, the results imply a lower adsorption energy for cesium on rhenium than expected. Further work should be done on rhenium to determine the ion current density-versus-temperature curves more conclusively. The surface ionization experiments on niobium show that niobium has a relatively low surface ionization efficiency and hence should not be considered as a potential ionizer material.

REFERENCES

1. M. Copely and T. Phipps, Phys. Rev., Vol. 48, 960, 1935
2. S. Datz and E. H. Taylor, J. Chem. Phys., Vol. 25, 389, 1956
3. S. V. Starodubtsev, J. Expt'l. Theoret. Phys., Vol. 19, 215, 1949
4. D. G. Worden, Progress in Astronautics and Rocketry (Academic Press, New York, 1961), Vol. 5, Electrostatic Propulsion, p. 141
5. Saul Dushman, Scientific Foundations of Vacuum Technique (John Wiley and Sons, Inc., New York, 1962), 2nd ed., J. M. Lafferty, Ed.
6. John B. Taylor and I. Langmuir, Phys. Rev., Vol. 44, 423, 1933
7. Jay Zemel, J. Chem. Phys, Vol. 28, 410, 1958
8. L. H. Taylor and H. H. Todd, Interim Summary Report, Contract NAS8-1537; Electro-Optical Systems, Inc. Report 1660-IR-1, Sept. 1962
9. A. L. Reimann, Phil. Mag., Vol. 25, 834, 1938
10. F. L. Hughes and H. Levinstein, Phys. Rev., Vol. 113, 1029, 1959
11. C. Agte, H. Alterthum, K. Becker, G. Heyne, and K. Moers, Zeits. f. anorg. allgem. Chemie, Vol. 196, 137, 1931
12. Roberto Levi and George A. Espersen, Phys. Rev., Vol. 78, 231, 1950
13. H. B. Wahlin and R. Sordahl, Phys. Rev., Vol. 45, 386, 1934
14. A. L. Riemann and Kerr-Grant, Phil. Mag., Vol. 22, 34, 1936
15. R. W. Griessel, General Electric Publication X-607, Sept. 1962
16. T. W. Hickmott and Gert Ehrlich, J. Phys. Chem. Solids, Vol. 5, 47, 1958
17. Joseph Eisinger, J. Chem. Phys., Vol. 28, 165, 1958
18. Gert Ehrlich, Annals N. Y. Acad. of Sciences, Vol. 101, 722, 1963
19. Gert Ehrlich, J. Phys. Chem., Vol. 60, 1388, 1956
20. J. A. Becker and C. D. Hartmann, J. Phys. Chem., Vol. 57, 157, 1953
21. Handbook of Chemistry and Physics (Chem. Rubber Pub. Co., Cleveland)
22. Gert Ehrlich, T. W. Hickmott, and F. G. Hudda, J. Chem. Phys. Vol. 28, 506, 1958
23. M. P. Hill and B. A. Pethica, J. Chem. Phys., Vol. 36, 3095, 1962

SUMMARY REPORT DISTRIBUTION LIST

Contract NAS3-2592

	Addressee	Number of Copies
1.	NASA-Lewis Research Center 21000 Brookpark Road Cleveland, Ohio 44135 Attention: Spacecraft Technology Procurement Section	1
2.	NASA-Lewis Research Center 21000 Brookpark Road Cleveland, Ohio 44135 Attention: Technology Utilization Office	1
3.	NASA-Lewis Research Center Spacecraft Technology Division 21000 Brookpark Road Cleveland, Ohio 44135 Attention: J. H. Childs Ross Hieber	2 19
4.	AFAPL (APIE) Wright-Patterson Air Force Base, Ohio Attention: Lt. Robert Supp	1
5.	NASA Headquarters FOB - 10B 600 Independence Avenue Washington, D. C. Attention: RNT/James Lazar	3
6.	AFWL Kirtland Air Force Base New Mexico Attention: WLPC/Capt. C. F. Ellis	1
7.	NASA Scientific & Technical Information Facility Box 5700 Bethesda 14, Maryland Attention: RQT-2448/NASA Representative	6
8.	NASA-Lewis Research Center 21000 Brookpark Road Cleveland, Ohio 44135 Attention: Library	2

	Addressee	Number of Copies
9.	NASA-Lewis Research Center 21000 Brookpark Road Cleveland, Ohio 44135 Attention: Reports Control	1
10.	Aerospace Corporation P. O. Box 95085 Los Angeles, California 90045 Attention: Library Technical Documents Group	1
11.	Westinghouse Astronuclear Laboratories Pittsburgh, Pennsylvania 15234 Attention: Mr. H. W. Szymanowski, Mgr. Electrical Propulsion Laboratory	1
12.	NASA-Lewis Research Center Electric Propulsion Laboratory 21000 Brookpark Road Cleveland, Ohio 44135 Attention: William R. Mickelsen	1